Noninvasive determination of the optical properties of two-layered turbid media

Alwin Kienle, Michael S. Patterson, Nora Dögnitz, Roland Bays, Georges Wagnières, and Hubert van den Bergh

Light propagation in two-layered turbid media having an infinitely thick second layer is investigated in the steady-state, frequency, and time domains. A solution of the diffusion approximation to the transport equation is derived by employing the extrapolated boundary condition. We compare the reflectance calculated from this solution with that computed with Monte Carlo simulations and show good agreement. To investigate if it is possible to determine the optical coefficients of the two layers and the thickness of the first layer, the solution of the diffusion equation is fitted to reflectance data obtained from both the diffusion equation and the Monte Carlo simulations. Although it is found that it is, in principle, possible to derive the optical coefficients of the two layers and the thickness of the first layer, we concentrate on the determination of the optical coefficients, knowing the thickness of the first layer. In the frequency domain, for example, it is shown that it is sufficient to make relative measurements of the phase and the steady-state reflectance at three distances from the illumination point to obtain useful estimates of the optical coefficients. Measurements of the absolute steady-state spatially resolved reflectance performed on two-layered solid phantoms confirm the theoretical results.

OCIS codes: 290.7050, 050.1960, 170.6930.

1. Introduction

In recent years great efforts have been made to determine the optical properties of biological tissue that can, in turn, be used to obtain knowledge of the physiological state of tissue. In almost all applications, models have been used that assume that the investigated tissue is homogeneous, but this assumption is often not valid. Instead, many parts of the body such as skin, esophagus, stomach, intestine, bladder, and head have a layered tissue structure. Thus, it is increasingly recognized that the results obtained from homogeneous models must be interpreted carefully[1,2] and that the theoretical models must be improved.

Using the diffusion approximation to the transport equation,[3] one can readily find solutions for a semi-infinite and homogeneous turbid medium in the steady-state, frequency, and time domains.[4–6] These equations can be used to obtain the optical properties by applying nonlinear regression to experimental data. For the semi-infinite geometry it is even possible to obtain the optical coefficients from the more exact transport equation using an approach that is based on scaling data from a single Monte Carlo simulation.[7] Monte Carlo simulations can also be used to calculate the light propagation in layered tissue,[8] but determination of the optical coefficients of two layers with this approach needs a high amount of computation time if used in an interative algorithm.[9,10] Although the solution of the diffusion equation for two layers is more complex than that for the semi-infinite medium, it offers much more rapid calculation than is possible with Monte Carlo simulations.

Several researchers have investigated the solution of the diffusion equation for layered turbid media. Takatani and Graham[11] and Schmitt *et al.*[12] derived analytical formulas for the steady-state reflectance by use of Green's functions to solve the diffusion equation, while Dayan *et al.*[13] applied Fourier and Laplace transforms to obtain expressions for the steady-state and the time-resolved reflectance. Keijzer *et al.*[14] and Schweiger *et al.*[15] employed a finite

A. Kienle, N. Dögnitz, R. Bays, G. Wagnières and H. van den Bergh are with the Institute of Environmental Engineering, Swiss Federal Institute of Technology, CH-1015 Lausanne, Switzerland. M. S. Patterson is with the Department of Medical Physics, Hamilton Regional Cancer Centre and McMaster University, 699 Concession Street, Hamilton, Ontario, L8V 5C2 Canada.

Received 19 May 1997; revised manuscript received 15 September 1997.

0003-6935/98/040779-13$10.00/0

element method and Cui and Ostrander[16] used a finite difference approach. A random walk model has been developed by Nossal *et al.*[17] However, these researchers did not compare their results to solutions of the transport equation, and the possibility of deriving the optical properties of the two layers from their models has not been studied.

In this article we solve the diffusion equation using the Fourier transform approach for a two-layered turbid medium having a semi-infinite second layer. Unlike Dayan *et al.*,[13] who introduced approximations to obtain relatively simple expressions for the reflectance, we avoided any approximation by calculating the reflectance using numerical integration. Moreover, the zero boundary condition was replaced by the more accurate extrapolated boundary condition.

We compare these solutions to Monte Carlo simulations in the steady-state, frequency, and time domains. Furthermore, by fitting the solutions of the diffusion equation to reflectance data obtained from the same equations to which typical experimental errors have been added, we attempt to solve the inverse problem and determine the optical properties of the two layers as well as the thickness of the first layer. To investigate whether the optical properties can also be derived if the solution of the diffusion equation is fitted to data from the more exact Monte Carlo method, nonlinear regressions were performed in the steady-state and frequency domains. For experimental confirmation of these theoretical results we measured the absolute steady-state spatially resolved reflectance on two-layered tissue phantoms.

We chose the values of the optical coefficients of the two layers and the thickness of the first layer of the investigated turbid media to resemble those that are especially relevant for two potential applications of the layered model: Near-infrared spectroscopy for measurements of cerebral oxygenation, where the thickness of the tissues above the brain is ~10 mm,[18] and optical noninvasive glucose monitoring, which has been investigated by measuring the steady-state spatially resolved reflectance on the abdomen,[19] where the thickness of the skin above the fat layer is approximately 2 mm.

2. Theory

A. Diffusion Equation

We derive the solutions of the diffusion equation for a two-layer medium for the steady-state reflectance (Subsection 2.A.1), for the phase and modulation of the reflectance in the frequency domain (Subsection 2.A.2), and for the time domain reflectance (Subsection 2.A.3). The first layer of the two-layer medium has a thickness l and the second layer is semi-infinite.

1. Steady-State Reflectance

Similar to Dayan *et al.*[13] we assume that an infinitely thin beam is incident perpendicular onto the turbid two-layer medium and that the beam is scattered isotropically in the upper layer at a depth of $z = z_0 = 1/(\mu_{s1}' + \mu_{a1})$, where μ_{si}' and μ_{ai} are the reduced scattering and the absorption coefficients of layer i, respectively. The origin of the coordinate system is the point where the beam enters the turbid medium and the z coordinate has the same direction as the incident beam. The x and y coordinates lie on the surface of the turbid sample and $\rho = (x^2 + y^2)^{1/2}$. Thus, the steady-state diffusion equation becomes

$$D_1\Delta\Phi_1(\mathbf{r}) - \mu_{a1}\Phi_1(\mathbf{r}) = -\delta(x, y, z - z_0), \qquad 0 \le z < l, \tag{1}$$

$$D_2\Delta\Phi_2(\mathbf{r}) - \mu_{a2}\Phi_2(\mathbf{r}) = 0, \qquad l \le z, \tag{2}$$

where $\mathbf{r} = (x, y, z)$. $D_i = 1/3(\mu_{ai} + \mu_{si}')$ and Φ_i are the diffusion constant and the fluence rate of layer i, respectively.

We solve these equations by the following steps. First the equations are transformed to ordinary differential equations with the use of a two-dimensional Fourier transform

$$\phi_i(z, s_1, s_2) = \int_{-\infty}^{\infty}\int_{-\infty}^{\infty} \Phi_i(x, y, z)\exp[i(s_1x + s_2y)]\mathrm{d}x\mathrm{d}y. \tag{3}$$

The derived equations are solved by use of the appropriate boundary conditions, and finally the results are inverse Fourier transformed to obtain the solution of Eqs. (1) and (2). Using Eq. (3), we obtain from Eqs. (1) and (2)

$$\frac{\partial^2}{\partial z^2}\phi_1(z, s) - \alpha_1^2\phi_1(z, s) = -\frac{1}{D_1}\delta(z - z_0), \qquad 0 \le z < l, \tag{4}$$

$$\frac{\partial^2}{\partial z^2}\phi_2(z, s) - \alpha_2^2\phi_2(z, s) = 0, \qquad l \le z, \tag{5}$$

where $\alpha_i^2 = (D_i s^2 + \mu_{ai})/D_i$ and $s^2 = s_1^2 + s_2^2$.

The following boundary conditions were employed to solve Eqs. (4) and (5):

$$\phi_1(-z_b, s) = 0, \tag{6}$$

$$\phi_2(\infty, s) = 0, \tag{7}$$

$$\frac{\phi_1(l, s)}{\phi_2(l, s)} = \frac{n_1^2}{n_2^2} = 1, \tag{8}$$

$$D_1\frac{\partial\phi_1(z, s)}{\partial z}\bigg|_{z=l} = D_2\frac{\partial\phi_2(z, s)}{\partial z}\bigg|_{z=l}. \tag{9}$$

Equation (6) states the extrapolated boundary condition for the tissue–air boundary.[5] Previously we compared different possible boundary conditions for a semi-infinite medium and found that Eq. (6) provides the best agreement between the diffusion equation

solution and Monte Carlo simulations.[6] The quantity z_b equals

$$z_b = \frac{1 + R_{\text{eff}}}{1 - R_{\text{eff}}} 2D_1. \tag{10}$$

R_{eff} represents the fraction of photons that is internally diffusely reflected at the boundary. R_{eff} was calculated according to Haskell *et al.*,[5] who found that R_{eff} equals 0.493 for a refractive index n of 1.4, which is representative of measured tissue data. In Eq. (8) we assumed that the refractive index n_i is the same for the first and the second layer. We solved Eqs. (4) and (5) by using Eqs. (6)–(9) and by considering the appropriate treatment of the Dirac function in Eq. (4). The results for $\phi_1(z, s)$ are

$$\phi_1(z, s) = \frac{\sinh[\alpha_1(z_b + z_0)]}{D_1\alpha_1} \times \frac{D_1\alpha_1 \cosh[\alpha_1(l - z)] + D_2\alpha_2 \sinh[\alpha_1(l - z)]}{D_1\alpha_1 \cosh[\alpha_1(l + z_b)] + D_2\alpha_2 \sinh[\alpha_1(l + z_b)]} - \frac{\sinh[\alpha_1(z_0 - z)]}{D_1\alpha_1}, \qquad 0 \le z < z_0, \tag{11}$$

$$\phi_1(z, s) = \frac{\sinh[\alpha_1(z_b + z_0)]}{D_1\alpha_1} \times \frac{D_1\alpha_1 \cosh[\alpha_1(l - z)] + D_2\alpha_2 \sinh[\alpha_1(l - z)]}{D_1\alpha_1 \cosh[\alpha_1(l + z_b)] + D_2\alpha_2 \sinh[\alpha_1(l + z_b)]}, \quad z_0 < z < l, \tag{12}$$

where we assumed that $l > z_0$, and for $\phi_2(z, s)$ we get

$$\phi_2(z, s) = \frac{\sinh[\alpha_1(z_b + z_0)]\exp[\alpha_2(l - z)]}{D_1\alpha_1 \cosh[\alpha_1(l + z_b)] + D_2\alpha_2 \sinh[\alpha_1(l + z_b)]}. \tag{13}$$

The two-dimensional Fourier inversion of Eqs. (11)–(13) is given by

$$\Phi_i(\rho, z) = \frac{1}{(2\pi)^2} \int_{\infty}^{\infty} \int_{\infty}^{\infty} \phi_i(z, s)\exp[-i(s_1x + s_2y)]\mathrm{d}s_1\mathrm{d}s_2 = \frac{1}{2\pi} \int_0^{\infty} \phi_i(z, s)sJ_0(s\rho)\mathrm{d}s, \tag{14}$$

where J_0 is the Bessel function of zeroth order. We performed this inverse transform numerically by applying Gauss's formula.[20] To check the obtained results, the Simpson formula for numerical integration was also programmed. The spatially resolved reflectance $R(\rho)$ is calculated as the integral of the radiance over the backward hemisphere[5]

$$R(\rho) = \int_{2\pi} d\Omega[1 - R_{\text{fres}}(\theta)] \times \frac{1}{4\pi}\left[\Phi_1(\rho, z = 0) + 3D_1 \frac{\partial\Phi_1(\rho, z = 0)}{\partial z} \cos\theta\right] \times \cos\theta, \tag{15}$$

where $R_{\text{fres}}(\theta)$ is the Fresnel reflection coefficient for a photon with an incident angle θ relative to the normal to the boundary. For a refractive index $n = 1.4$, Eq. (15) gives[6]

$$R(\rho) = 0.118\Phi_1(\rho, z = 0) + 0.306D_1 \frac{\partial}{\partial z} \Phi_1(\rho, z)|_{z=0}. \tag{16}$$

In Subsection 4.C a semi-infinite model is also used to fit the steady-state spatially resolved reflectance from two-layered media. Equation (8) from Ref. 6 is applied, which is identical to Eq. (16) from this article for $\mu_{a1} = \mu_{a2}$ and $\mu_{s1}' = \mu_{s2}'$.

2. *Frequency Domain Reflectance*

In the frequency domain method the source is sinusoidally modulated at frequency f. Thus the measured signal at the detector is also sinusoidal but the oscillation is delayed and the modulation is reduced. The interesting quantities in the frequency domain are the phase angle θ between the source and the detected signal and the modulation M:

$$\theta = \tan^{-1} \frac{\text{Im}[R(\rho, \omega)]}{\text{Re}[R(\rho, \omega)]}, \tag{17}$$

$$M = \left\{\frac{\text{Im}[R(\rho, \omega)]^2 + \text{Re}[R(\rho, \omega)]^2}{\text{Re}[R(\rho, \omega = 0)]^2}\right\}^{1/2}, \tag{18}$$

where $\omega = 2\pi f$.

The real and imaginary parts of the reflectance $R(\rho, \omega)$ can be obtained by using the formula for $R(\rho)$ in Subsection 2.A.1, but α_i has now to be computed with $\alpha_i^2 = (D_i s^2 + \mu_{ai} + j\omega/c)/D_i$. The velocity of light in the medium is c and $j = (-1)^{1/2}$.

In this article the investigated quantities for measurements in the frequency domain are the phase and steady-state reflectance because the use of these quantities is often superior to the use of the phase and modulation for the determination of the optical coefficients.[21,22] In Subsection 4.C we also use a semi-infinite model to fit the phase and the steady-state reflectance from two-layered media. Equations (1) and (3) from Ref. 22 are applied, which are identical to Eqs. (15) and (16) of this article for $\mu_{a1} = \mu_{a2}$ and $\mu_{s1}' = \mu_{s2}'$.

3. *Time Domain Reflectance*

The time domain reflectance $R(\rho, t)$ can be derived by the Fourier and Laplace transforming Eq. (11).[13] A different approach has been used here. The real and

imaginary parts of the reflectance in the frequency domain $R(\rho, \omega)$, (see Subsection 2.A.2) were calculated at many frequencies. To obtain the time domain reflectance these data were fast Fourier transformed. We checked these results by comparing $R(\rho, t)$ for a semi-infinite turbid medium using $\mu_{s1}' = \mu_{s2}'$ and $\mu_{a1} = \mu_{a2}$ in Eqs. (11) and (12) with the time domain reflectance obtained from the diffusion equation for a semi-infinite medium [Eq. (8) in Ref. 6].

B. Monte Carlo Simulations

The solutions of the diffusion equation are compared (Subsection 4.A) and fitted (Subsection 4.C) to Monte Carlo simulations. The principles of Monte Carlo simulation of photon transport in turbid media have been described elsewhere,[23,24] so that we mention only the salient features of our Monte Carlo program. A pencil photon beam was normally incident onto the two-layered turbid medium. For calculation of the scattering angle we used the Henyey-Greenstein[25] phase function. The refractive index was equal to 1.4 for both layers. The Monte Carlo simulations were performed in the time domain. The steady-state reflectance and the phase were calculated from the time domain reflectance using the fast Fourier transform. For the Monte Carlo simulations in the time domain a spatial resolution of 0.5 or 1.0 mm and a temporal resolution of 2.5 ps for $t < 100$ ps and of 10 ps for 100 ps $< t <$ 4000 ps were chosen for scoring the reflectance. This ensures that all essential information about $R(\rho, t)$ is obtained from the simulations, and errors are avoided when the steady-state and frequency domain reflectance are calculated. The anisotropy factor g was chosen to be 0.8, because the variation in g between 0.8 and 1 does not change the reflectance significantly as long as μ_s' is constant.[7] For investigations of the turbid media with thicknesses of the first layer of 6 and 10 mm, $R(\rho, t)$ was calculated for different absorption coefficients in the second layer from only one simulation by scoring the lengths of the photon paths in the second layer and applying Beer's law.[26,7]

For the nonlinear regression a combination of the gradient search method and the method of linearizing the fitting function was used.[27] The logarithm of the absolute reflectance was fitted in the nonlinear regressions for both the investigations in the time domain and in the steady-state domain. For the investigations in the frequency domain, relative phase values (the phase difference determined at adjacent distances) and relative steady-state reflectance (the ratio determined at adjacent distances) were used. Equal weights for all data points were applied in the fitting procedure.

3. Materials and Methods

Absolute steady-state spatially resolved reflectance measurements were performed in a similar way to those described in detail previously.[28] Briefly, light from a He–Ne laser at $\lambda = 543$ nm or at $\lambda = 612$ nm was incident approximately perpendicular onto the tissue phantoms. The diffusely reflected photons were imaged onto a CCD camera and the intensity values were recorded. From these, the spatially resolved reflectance was calculated. To make absolute measurements it is necessary to calibrate the detector response. This was done by measuring the reflectance profile for a homogeneous Liposyn phantom with known optical properties. By measuring the source power and calculating the theoretical reflectance, we determined the detector response.

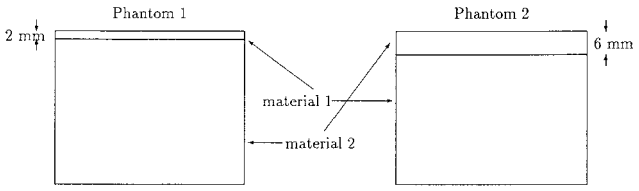

Fig. 1. Scheme of the manufactured phantoms.

The measurements of the spatially resolved reflectance were made on two-layered tissue phantoms. The principles of the manufacturing process are described in Ref. 29. The basic medium is a two-component transparent silicone that cures at room temperature. The refractive index of the silicone is close to 1.4.[29] Before the base and the catalyst were mixed, the scattering and absorbing particles were added. We used polystyrene spheres with a 2.5-μm diameter dispersed in ethanol as scattering material and graphite powder (also dispersed in ethanol) as absorbing material. These components were mixed in the silicone and heated at $\sim$100 °C for several hours to remove the ethanol. If the ethanol is incompletely removed, bubbles can be formed during the curing process.

Two two-layered phantoms were manufactured, one consisting of a 2-mm-thick and the other of a 6-mm-thick first layer. Two silicon mixtures were made, each with different optical properties. One of these was used for the first layer of phantom 1 and for the second layer of phantom 2. The other mixture was used for the first layer of phantom 2 and the second layer of phantom 1 (see Fig. 1). Therefore, it was possible to determine the optical properties of the layers separately by measuring the absolute spatially resolved reflectance at the sides of the second layers of the phantoms. In these measurements the first layer does not influence the light propagation, and thus the solution of the diffusion equation for a semi-infinite medium can be applied. The lateral dimensions of the smaller of the two phantoms were 9 cm $\times$ 9 cm and the height was 6 cm. This is large enough to eliminate any influence of the lateral boundaries.

4. Results

In this section we first present results comparing the solutions of the diffusion equation derived in Subsection 2.A to Monte Carlo simulations in the steady-state, frequency, and time domains (Subsection 4.A). This is followed by two subsections in which the possibility of extracting information about the two-layer

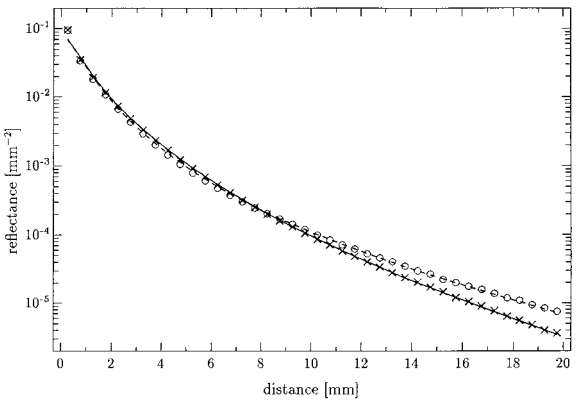

Fig. 2. Comparison of the steady-state spatially resolved reflectance calculated with Eq. (16) (lines) to Monte Carlo simulations (symbols). The optical parameters of the two-layered turbid media are $\mu_{a1} = 0.02\ \text{mm}^{-1}$, $\mu_{s1}' = 1.3\ \text{mm}^{-1}$, $\mu_{a2} = 0.01\ \text{mm}^{-1}$, and $\mu_{s2}' = 1.2\ \text{mm}^{-1}$ (solid curve, crosses) or $\mu_{s2}' = 0.7\ \text{mm}^{-1}$ (dashed curve, circles). The thickness of the first layer is $l = 2$ mm and $n = 1.4$.

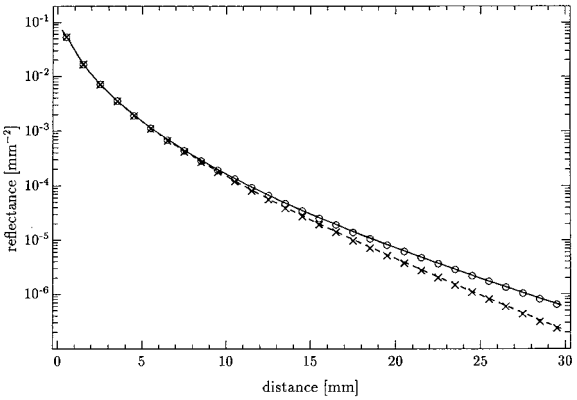

Fig. 3. Comparison of the steady-state spatially resolved reflectance calculated with Eq. (16) (lines) to Monte Carlo simulations (symbols). The optical parameters of the two-layered turbid media are $\mu_{s1}' = 1.3\ \text{mm}^{-1}$, $\mu_{a1} = 0.005\ \text{mm}^{-1}$, $\mu_{s2}' = 1.0\ \text{mm}^{-1}$, and $\mu_{a2} = 0.01\ \text{mm}^{-1}$ (solid curve, circles) or $\mu_{a2} = 0.022\ \text{mm}^{-1}$ (dashed curve, crosses). The thickness of the first layer is $l = 6$ mm and $n = 1.4$.

medium predominantly by measurements in the steady-state and frequency domains is studied. The optical coefficients of the two-layered medium were determined by fitting the diffusion solutions to reflectance data calculated with the diffusion equation (Subsection 4.B) or with the Monte Carlo method (Subsection 4.C). Finally, we present the results obtained from the measurements of the absolute steady-state spatially resolved reflectance from two-layered phantoms (Subsection 4.D).

A. Comparison with Monte Carlo Simulations

In our comparison of the solutions of the diffusion equation to Monte Carlo simulations, the reflectance is compared for media having optical coefficients that are used in Subsection 4.C. Figure 2 shows the steady-state reflectance $R(\rho)$ for $\mu_{a1} = 0.02\ \text{mm}^{-1}$, $\mu_{s1}' = 1.3\ \text{mm}^{-1}$, $\mu_{a2} = 0.01\ \text{mm}^{-1}$, and $\mu_{s2}' = 1.2\ \text{mm}^{-1}$ or $\mu_{s2}' = 0.7\ \text{mm}^{-1}$. The thickness of the first layer is $l = 2$ mm. In general, $R(\rho)$ calculated with the diffusion equation is close to the Monte Carlo data (the differences are smaller than 7% for distances greater than 1.25 mm). This is not the case for distances close to the source, where it is known that the diffusion approximation is not valid. The different behavior of the reflectance for the media with different μ_{s2}' can be explained as follows. For small distances ($\rho < 2$ mm) the influence of the second layer is minimal and therefore the reflectance is similar. For long distances ($\rho > 8$ mm) the reflectance from the turbid medium with $\mu_{s2}' = 0.7\ \text{mm}^{-1}$ is greater than from that with $\mu_{s2}' = 1.2\ \text{mm}^{-1}$, because the smaller reduced scattering coefficient of the second layer allows the light to travel further away from the incident beam. For intermediate distances the greater reflectance for the medium with $\mu_{s2}' = 1.2\ \text{mm}^{-1}$ is caused by the enhanced remitted photons from the second layer due to the higher reduced scattering coefficient of the second layer.

In Figs. 3 and 4 the steady-state spatially resolved reflectance for two-layered media with thicknesses of the first layer of 6 and 10 mm, respectively, are shown. The optical parameters are $\mu_{s1}' = 1.3\ \text{mm}^{-1}$, $\mu_{a1} = 0.005\ \text{mm}^{-1}$, $\mu_{s2}' = 1.0\ \text{mm}^{-1}$, and $\mu_{a2} = 0.01\ \text{mm}^{-1}$ or $\mu_{a2} = 0.022\ \text{mm}^{-1}$. For these parameters the solutions of the diffusion equation are also close to the Monte Carlo simulations. For small distances the curves for different μ_{a2} are similar, because the reflectance is not influenced by the optical properties of the second layer. Because of the greater absorption coefficient of the second layer of the medium with $\mu_{a2} = 0.022\ \text{mm}^{-1}$ the reflectance is smaller at large distances values compared with the turbid medium with $\mu_{a2} = 0.01\ \text{mm}^{-1}$. The distance from the source where the reflectance of the medium with the greater μ_{a2} has a noticeablely smaller re-

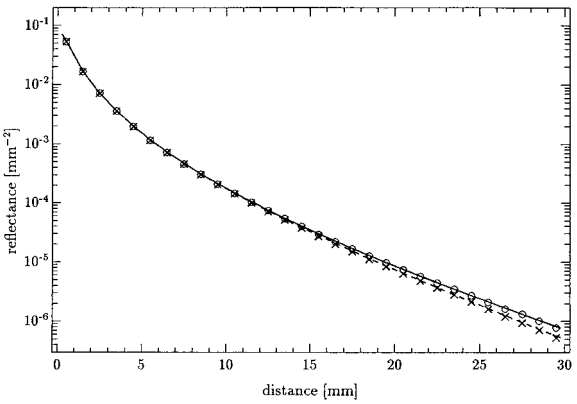

Fig. 4. Comparison of the steady-state spatially resolved reflectance calculated with Eq. (16) (curves) to Monte Carlo simulations (symbols). The optical parameters of the two-layered turbid media are $\mu_{s1}' = 1.3\ \text{mm}^{-1}$, $\mu_{a1} = 0.005\ \text{mm}^{-1}$, $\mu_{s2}' = 1.0\ \text{mm}^{-1}$, and $\mu_{a2} = 0.01\ \text{mm}^{-1}$ (solid curve, circles) or $\mu_{a2} = 0.022\ \text{mm}^{-1}$ (dashed curve, crosses). The thickness of the first layer is $l = 10$ mm and $n = 1.4$.

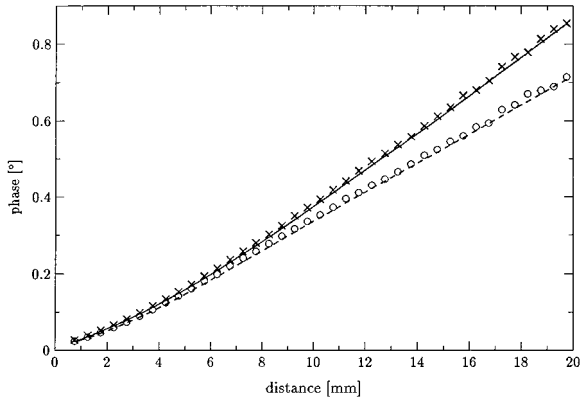

Fig. 5. Comparison of the phase versus distance calculated with Eq. (17) (curves) to Monte Carlo simulations (symbols). The optical parameters of the two-layered turbid media are $n = 1.4$, $\mu_{a1} = 0.02\ \text{mm}^{-1}$, $\mu_{s1}' = 1.3\ \text{mm}^{-1}$, $\mu_{a2} = 0.01\ \text{mm}^{-1}$, and $\mu_{s2}' = 1.2\ \text{mm}^{-1}$ (solid curve, crosses) or $\mu_{s2}' = 0.7\ \text{mm}^{-1}$ (dashed curve, circles). The thickness of the first layer is $l = 2$ mm and the modulation frequency is $f = 195$ MHz.

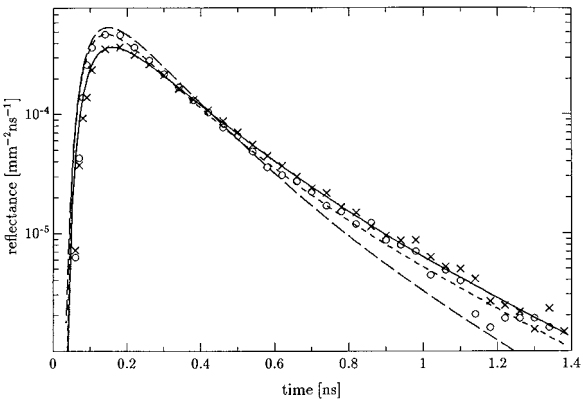

Fig. 6. Comparison of the time-resolved reflectance calculated with the diffusion theory (curves) to Monte Carlo simulations (symbols). The optical parameters of the two-layered turbid media are $n = 1.4$, $\mu_{a1} = 0.02\ \text{mm}^{-1}$, $\mu_{s1}' = 1.3\ \text{mm}^{-1}$, $\mu_{a2} = 0.01\ \text{mm}^{-1}$, and $\mu_{s2}' = 1.2\ \text{mm}^{-1}$ (solid curve, crosses) or $\mu_{s2}' = 0.7\ \text{mm}^{-1}$ (dashed curve, circles). The thickness of the first layer is $l = 2$ mm, and the distance is $\rho = 9.75$ mm. The time-resolved reflectance calculated with the solution proposed by Dayan *et al*. is also shown for the medium with $\mu_{s2}' = 0.7\ \text{mm}^{-1}$ (long dashed curve).

flectance than the medium with the smaller μ_{a2} is greater when the top layer is thicker (compare Fig. 3 with Fig. 4). These figures show also that the difference between the reflectance for media of different μ_{a2} is greater for $l = 6$ mm than for $l = 10$ mm. Consequently, one has to measure at greater distances to obtain the optical coefficients from media having a thicker first layer.

For the determination of the optical coefficients in the frequency domain (Subsections 4.B and 4.C) the measurement of the steady-state reflectance and the phase is assumed. Figure 5 compares the phase calculated with Eq. (17) with that obtained from Monte Carlo simulations. The optical coefficients and the thickness of the first layer are those that have been used in Fig. 2. The modulation frequency is $f = 195$ MHz. The phase values from the turbid medium with the greater reduced scattering coefficient in the second layer are greater than those from the other medium. The phase obtained from the diffusion equation has a systematically lower value than the Monte Carlo data. Similar differences can also be observed with the solutions of the diffusion equation for the semi-infinite geometry. In Subsections 4.B and 4.C we use the phase difference determined at different distances to determine the optical coefficients. In this way a considerable part of these differences is canceled out.

To compare the time-resolved reflectance from these two-layered media the solution of the diffusion equation was obtained by calculating the real part and the imaginary part of $R(\rho, \omega)$ at 512 different frequencies (97.7 MHz, 195 MHz, . . . , 50 GHz) and by fast Fourier transforming these data. The reflectance at $\rho = 9.75$ mm can be seen in Fig. 6. The results calculated with the diffusion theory are within the statistical errors of the Monte Carlo data for times longer than $t = 0.2$ ns. The differences at shorter times are caused by the failure of the diffusion approximation for photons that have been minimally scattered. The time-resolved reflectance for the medium with $\mu_{s2}' = 0.7\ \text{mm}^{-1}$ calculated with the solution proposed by Dayan *et al*. is also shown in the figure [long dashed curve, Eqs. (12) and (25) in Ref. 13]. It can be seen that this solution does not match the Monte Carlo data owing to the approximations made in its derivation.

B. Determination of the Optical Coefficients from Nonlinear Regressions to Solutions of the Diffusion Equation

To investigate what information can be obtained from measurements of the reflectance from a two-layered medium in the steady-state, frequency, and time domains if no approximations in the theoretical description are made, we used the solutions presented in Subsection 2.A for nonlinear regressions to data that were calculated with the same equations and to which typical experimental errors were added. Errors of 1% and 0.1° were assumed for the measurement of the steady-state reflectance and the phase. We found that for measurements of the absolute steady-state spatially resolved reflectance it is possible to determine μ_s' and μ_a for both layers if the thickness of the first layer is known and the distance range of the measurements of $R(\rho)$ is suitable. This confirms the results that we obtained in a previous study[10] where Monte Carlo simulations were used or the solution of the diffusion equation described by Schmitt *et al*.[12] For a first layer thickness of 2 mm, measurement errors in $R(\rho)$ in the range of 1% result in errors of typically 10–20% in μ_{a1}, μ_{s2}', μ_{a2}, whereas μ_{s1}' can be determined with an accuracy of better than 5%. Uncertainties in l of the order of 10% give similar errors in the determination of the

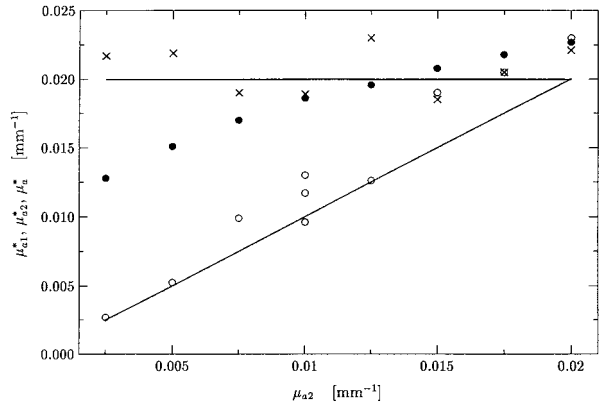

Fig. 7. Estimated absorption coefficients of the first (μ_{a1}*, crosses) and second layer (μ_{a2}*, open circles) determined by nonlinear regressions of Eq. (16) to Monte Carlo data are shown versus the true absorption coefficient of the second layer used in the Monte Carlo simulations (μ_{a2}). The optical parameters of the Monte Carlo simulations are $\mu_{s1}' = 1.3$ mm^{-1}, $\mu_{a1} = 0.02$ mm^{-1}, $\mu_{s2}' = 1.0$ mm^{-1}, and μ_{a2} is varied between $\mu_{a2} = 0.0025$ mm^{-1} and $\mu_{a2} = 0.02$ mm^{-1}. The thickness of the first layer is $l = 2$ mm. The lines indicate the correct values. Also shown are the absorption coefficients (μ_a*) obtained from nonlinear regressions to the two-layer Monte Carlo data using a diffusion solution that assumes a semi-infinite medium (solid circles). Reflectance data at distances $\rho = 1.25, 1.75, \ldots, 17.75$ mm were used in the nonlinear regression.

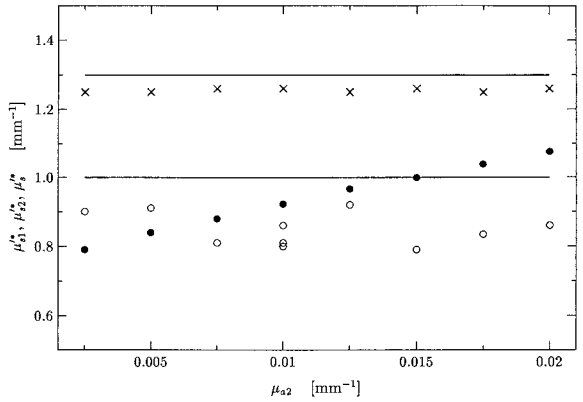

Fig. 8. Estimated reduced scattering coefficients of the first (μ_{s1}'*, crosses) and second layer (μ_{s2}'*, open circles) determined by nonlinear regressions of Eq. (16) to Monte Carlo data are shown versus the absorption coefficient of the second layer used in the Monte Carlo simulations (μ_{a2}). The optical parameters of the Monte Carlo simulations are $\mu_{s1}' = 1.3$ mm^{-1}, $\mu_{a1} = 0.02$ mm^{-1}, $\mu_{s2}' = 1.0$ mm^{-1}, and μ_{a2} is varied between $\mu_{a2} = 0.0025$ mm^{-1} and $\mu_{a2} = 0.02$ mm^{-1}. The thickness of the first layer is $l = 2$ mm. The lines indicate the correct values. Also shown are the reduced scattering coefficients (μ_s'*) obtained from nonlinear regressions to the two-layer Monte Carlo data using a diffusion solution that assumes a semi-infinite medium (solid circles). Reflectance data at distances $\rho = 1.25, 1.75, \ldots, 17.75$ mm were used in the nonlinear regression.

optical coefficients. If the thickness of the first layer is not known, i.e., if five parameters are fitted, it is possible to get reasonable values of the optical coefficients and l when the starting parameters of the nonlinear regression are not too far from the real ones. We note that these quantitive data depend on the number of points at which $R(\rho)$ is measured. (Here, typically, reflectance data at approximately 20 or 40 distances located between $\rho = 1$ mm and $\rho = 20$ mm were used.)

In the frequency domain it is also, in principle, possible to determine μ_s' and μ_a of the two layers and the thickness of the first layer. However this is true only if the start parameters of the nonlinear regressions are not too far from the real ones. In addition, it was found that the convergence of the nonlinear regression was often slow. We also investigated the determination of μ_s' and μ_a when the thickness of the first layer was known. We found that it is sufficient to measure the phase and steady-state reflectance at three distances to obtain the correct optical coefficients. Here it was assumed that the phase difference and the steady-state reflectance ratio are determined between the first and the second and between the second and the third distances. We added typical errors for the measurements of the phase and the intensity and found that the obtained optical coefficients are quite stable. This was also the case when the thickness of the first layer was known only within an error of 10%. For example, for $l = 6$ mm and measurement positions at 7.5, 13.5, and 19.5 mm and with optical coefficients similar to those in Subsection 4.A, the errors in the derived absorption and reduced scattering coefficients were ~10% or less assuming measurement errors of 0.1° in the phase and 1% in the steady-state reflectance. Similar errors were obtained when assumptions of $l = 5.4$ mm or $l = 6.6$ mm were used in the nonlinear regression to reflectance data generated for a medium with $l = 6$ mm.

In the time domain it was found that it is possible to determine μ_s' and μ_a for both layers from absolute time-resolved reflectance measured at one distance if the thickness of the first layer is known.

C. Determination of the Optical Coefficients from Nonlinear Regressions to Monte Carlo Simulations

To determine the optical properties with the use of nonlinear regressions to Monte Carlo data, we concentrate here on the steady-state domain and frequency domain reflectance, because the time domain calculations are relatively time-consuming. We described above the possibility of obtaining not only the optical parameters of the two layers but also the thickness of the first layer if the theoretical model contains no approximations (a solution of the diffusion equation was fitted to data from this solution plus noise). However, if the solution of the diffusion equation is used to fit Monte Carlo data or experiments, a systematic error is introduced. In this case it is difficult to obtain good estimates of all five parameters. Thus, in the following it is assumed that the thickness of the first layer is known.

1. Steady-State Domain

We first present the optical coefficients obtained by fitting the solution of the diffusion equation to Monte

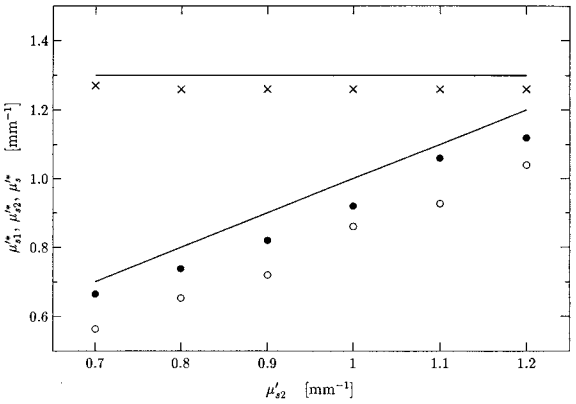

Fig. 9. Estimated reduced scattering coefficients of the first ($\mu_{s1}'^*$, crosses) and second layer ($\mu_{s2}'^*$, open circles) determined by nonlinear regressions of Eq. (16) to Monte Carlo data are shown versus the reduced scattering coefficient of the second layer used in the Monte Carlo simulations (μ_{s2}'). The optical parameters of the Monte Carlo simulations are $\mu_{a1} = 0.02$ mm^{-1}, $\mu_{s1}' = 1.3$ mm^{-1}, $\mu_{a2} = 0.01$ mm^{-1}, and μ_{s2}' is varied between $\mu_{s2}' = 0.7$ mm^{-1} and $\mu_{s2}' = 1.2$ mm^{-1}. The thickness of the first layer is $l = 2$ mm. The lines indicate the correct values. Also shown are the reduced scattering coefficients ($\mu_s'^*$) obtained from nonlinear regressions to the two-layer Monte Carlo data using a diffusion solution that assumes a semi-infinite medium (solid circles). Reflectance data at distances $\rho = 1.25, 1.75, \ldots, 19.75$ mm were used in the nonlinear regression.

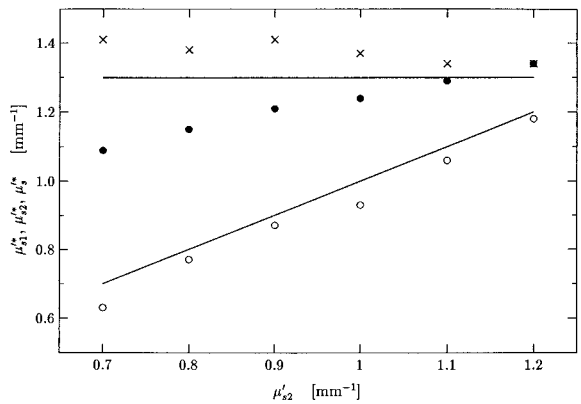

Fig. 10. Estimated reduced scattering coefficients of the first ($\mu_{s1}'^*$, crosses) and second layer ($\mu_{s2}'^*$, open circles) determined by nonlinear regressions of Eqs. (16) and (17) to Monte Carlo data are shown versus the reduced scattering coefficient of the second layer used in the Monte Carlo simulations (μ_{s2}'). The optical parameters of the Monte Carlo simulations are $\mu_{a1} = 0.02$ mm^{-1}, $\mu_{s1}' = 1.3$ mm^{-1}, $\mu_{a2} = 0.01$ mm^{-1}, and μ_{s2}' is varied between $\mu_{s2}' = 0.7$ mm^{-1} and $\mu_{s2}' = 1.2$ mm^{-1}. The thickness of the first layer is $l = 2$ mm. The lines indicate the correct values. The frequency domain reflectance at distances $\rho = 3.75, 6.75, 9.75$ mm were used in the nonlinear regression and the modulation frequency is $f = 195$ MHz. Also shown are the reduced scattering coefficients ($\mu_s'^*$) obtained from nonlinear regressions to the two-layer Monte Carlo data using a diffusion solution that assumes a semi-infinite medium (solid circles).

Carlo data for a two-layered medium consisting of a 2-mm-thick first layer. The optical coefficients used in the Monte Carlo simulations are $\mu_{s1}' = 1.3$ mm^{-1}, $\mu_{a1} = 0.02$ mm^{-1}, $\mu_{s2}' = 1.0$ mm^{-1}, and μ_{a2} is varied between $\mu_{a2} = 0.0025$ mm^{-1} and $\mu_{a2} = 0.02$ mm^{-1}. Figures 7 and 8 show the absorption and reduced scattering coefficients, respectively, which were obtained from the nonlinear regressions. These graphs show that it is possible to obtain the four optical coefficients from absolute spatially resolved reflectance measurements by using the solution of the diffusion equation in the nonlinear regression. The reduced scattering coefficient of the first layer can be determined quite accurately, while μ_{a1}, μ_{s2}', and μ_{a2} show differences of typically 10–30% compared with the correct values. These deviations are caused by both the statistical uncertainty in the Monte Carlo results and the systematic errors introduced by the diffusion approximation. To demonstrate the former, μ_{a2}^* and $\mu_{s2}'^*$ obtained from nonlinear regression to three independent Monte Carlo simulations calculated with $\mu_{a2} = 0.01$ mm^{-1} are shown in Figs. 7 and 8. About five million photons were used in the simulations resulting in an error in $R(\rho)$ of ~2% at distances greater than $\rho = 15$ mm. This results in an uncertainty in the determination of μ_{a2} and μ_{s2}' of ~10–20%. In contrast, the reduced scattering and absorption coefficients determined from the nonlinear regression using a solution of the diffusion equation for a semi-infinite medium show a change smaller than 1% when different Monte Carlo simulations are fitted. However, the derived optical coefficients give little information about the true optical coefficients. As we reported in an earlier study, in some cases the estimate is not even between the true values for the top and bottom layers.[10]

Figure 9 shows the reduced scattering coefficients derived from nonlinear regressions to Monte Carlo reflectance data from a two-layered medium having the same optical parameters in the first layer as the case discussed above. However, $\mu_{a2} = 0.01$ mm^{-1} was now held constant and μ_{s2}' was varied between $\mu_{s2}' = 0.7$ mm^{-1} and $\mu_{s2}' = 1.2$ mm^{-1}. The thickness of the first layer was 2 mm. The reduced scattering coefficient of the first layer can be determined with errors less than 5%, whereas the estimates of μ_{s2}' are ~0.15 mm^{-1} too low. The figure indicates that the errors arising from the diffusion approximation are greater than those produced from the statistical uncertainty of the Monte Carlo results. The errors in determining μ_{a1} and μ_{a2} are smaller than 10% and 30%, respectively (data not shown).

Investigations of the turbid media with thicknesses of the first layer of 6 and 10 mm showed that the errors in deriving the optical coefficients by use of absolute steady-state spatially resolved reflectance were greater than for $l = 2$ mm. We found for media with $l = 6$ mm, $\mu_{s1}' = 1.3$ mm^{-1}, $\mu_{a1} = 0.005$ mm^{-1}, $\mu_{s2}' = 1.0$ mm^{-1}, and μ_{a2} between $\mu_{a2} = 0.01$ mm^{-1} and $\mu_{a2} = 0.026$ mm^{-1}, that μ_{s1}' can be derived within an error of 3% and that the errors in the other coefficients are approximately 50% when reflectance values for distances up to $\rho = 30$ mm are used. For media with the same optical coefficients and $l = 10$

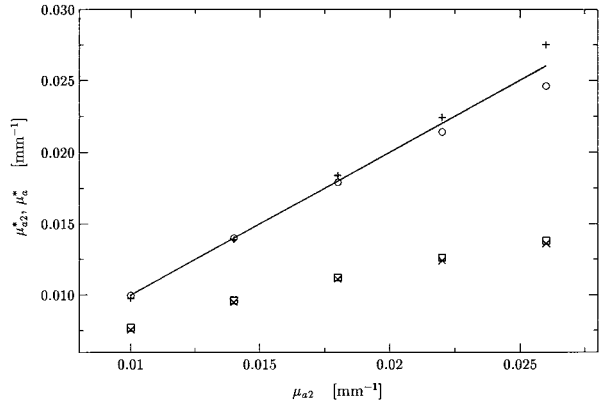

Fig. 11. Estimated absorption coefficients of the second layer (μ_{a2}*, open circles, pluses) determined by nonlinear regressions of Eqs. (16) and (17) to Monte Carlo data are shown versus the absorption coefficient of the second layer used in the Monte Carlo simulations (μ_{a2}). The optical parameters of the Monte Carlo simulations are $\mu_{s1}' = 1.3$ mm^{-1}, $\mu_{a1} = 0.005$ mm^{-1}, $\mu_{s2}' = 1.0$ mm^{-1}, and μ_{a2} is varied between $\mu_{a2} = 0.01$ mm^{-1} and $\mu_{a2} = 0.025$ mm^{-1}. The thickness of the first layer is $l = 6$ mm. The line indicates the correct values. Also shown is the absorption coefficient (μ_a*, crosses, boxes) obtained from nonlinear regressions to the two-layer Monte Carlo data when a diffusion solution that assumes a semi-infinite medium is used. The frequency domain reflectance at distances $\rho = 7.5, 13.5, 19.5$ mm were used in the nonlinear regression and the modulation frequency is $f = 195$ MHz. Two independent Monte Carlo simulations were performed.

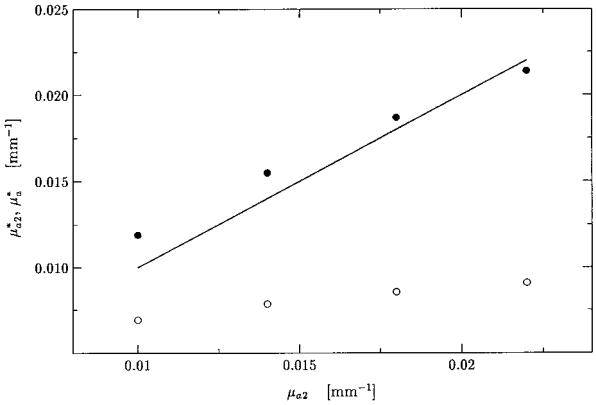

Fig. 12. Estimated absorption coefficients of the second layer (μ_{a2}*, solid circles) determined by nonlinear regressions of Eqs. (16) and (17) to Monte Carlo data are shown versus the absorption coefficient of the second layer used in the Monte Carlo simulations (μ_{a2}). The optical parameters of the Monte Carlo simulations are $\mu_{s1}' = 1.3$ mm^{-1}, $\mu_{a1} = 0.005$ mm^{-1}, $\mu_{s2}' = 1.0$ mm^{-1}, and μ_{a2} is varied between $\mu_{a2} = 0.01$ mm^{-1} and $\mu_{a2} = 0.022$ mm^{-1}. The thickness of the first layer is $l = 10$ mm. The line indicates the correct values. Also shown is the absorption coefficient (μ_a*, open circles) obtained from nonlinear regressions to the two-layer Monte Carlo data when a diffusion solution that assumes a semi-infinite medium is used. The frequency domain reflectance at distances $\rho = 7.5, 18.5, 29.5$ mm were used in the nonlinear regression and the modulation frequency is $f = 195$ MHz.

mm the errors in the optical coefficients of the second layer are even greater.

2. *Frequency Domain*

Figure 10 shows the reduced scattering coefficient estimated from frequency domain data for the same Monte Carlo simulations that have been used in Fig. 9. The phase difference and the steady-state reflectance ratio between $\rho = 3.75$ mm and $\rho = 6.75$ mm and between $\rho = 6.75$ mm and $\rho = 9.75$ mm are used in the nonlinear regression. The modulation frequency is $f = 195$ MHz, as in all results for this subsection. Also shown is the reduced scattering coefficient derived by employing a solution for the semi-infinite medium. In this case the phase difference and the steady-state reflectance ratio between $\rho = 3.75$ mm and $\rho = 9.75$ mm are used in the nonlinear regression.

Whereas μ_{s1}' can be determined less accurately than in the steady-state domain, better estimates of μ_{s2}' are obtained. The errors in determining μ_{a2} are typically smaller than 10% and μ_{a1} can be determined with an error of typically 30–40% (data not shown). The reduced scattering coefficient determined from the semi-infinite model is usually between μ_{s1}' and μ_{s2}'.

Figures 11 and 12 show μ_{a2} derived from nonlinear regressions to Monte Carlo reflectance data from two-layered turbid media with first layer thicknesses of 6 and 10 mm, respectively. The optical parameters of the Monte Carlo simulations are $\mu_{s1}' = 1.3$ mm^{-1}, $\mu_{a1} = 0.005$ mm^{-1}, $\mu_{s2}' = 1.0$ mm^{-1}, and μ_{a2} is varied between $\mu_{a2} = 0.01$ mm^{-1} and $\mu_{a2} = 0.026$ mm^{-1} ($\mu_{a2} = 0.022$ mm^{-1} in Fig. 12). The data from two independent Monte Carlo simulations are shown in Fig. 11. The reflectance for the media with different μ_{a2} values were calculated from one Monte Carlo simulation as explained in Subsection 2.B. Frequency domain reflectance data at $\rho = 7.5$, 13.5, and 19.5 mm were used in the analysis. The absorption coefficients derived from a semi-infinite model are also shown. In this case the phase difference and the reflectance ratio between $\rho = 7.5$ mm and $\rho = 19.5$ mm ($\rho = 29.5$ mm in Fig. 12) are used in the nonlinear regression.

It can be seen from Fig. 11 that the absorption coefficient of the second layer can be derived quite accurately. The errors increase with an increasing absorption coefficient, probably because fewer detected photons have passed through the second layer. The results for the two different Monte Carlo simulations show that the errors at large μ_{a2} values are due to the statistical uncertainty in the Monte Carlo results. For these simulations approximately 10 million photons were used, which resulted in uncertainties in the phase of ~0.1° and in the steady-state reflectance of ~1% at $\rho = 19.75$ mm. The errors in the derived μ_{s1}', μ_{s2}', and μ_{a1} are smaller than 1%, 10%, and 15%, respectively, (figure not shown).

In Fig. 12 the results of one independent Monte Carlo simulation are shown. The absorption coefficients of the second layer can be derived within an error of 20%. The errors in μ_{s1}', μ_{s2}', and μ_{a1} are smaller than 1%, 20%, and 20%, respectively, (figure

Table 1. Optical Coefficients of the Two-Layered Medium (Phantom 1) Having a First Layer Thickness of $l = 2$ mm Derived from Measurements on the Side of Phantom 1 and 2 (Semi-Infinite Media) and on the Top (Two-Layered Media) at 543 and 612 nm

Phantom 1	λ [nm]	μ_{s1}' [mm^{-1}]	μ_{a1} [mm^{-1}]	μ_{s2}' [mm^{-1}]	μ_{a2} [mm^{-1}]
Semi-infinite	543	0.52	0.024	1.05	0.009
Two-layer	543	0.43	0.035	0.80	0.007
Semi-infinite	612	0.50	0.025	1.05	0.008
Two-layer	612	0.47	0.025	0.85	0.015

not shown). Although 50 million photons were used for these Monte Carlo simulations, the uncertainties are quite large at distances of approximately 25–30 mm. Therefore, the errors in the derived optical properties are probably mainly due to the uncertainties in the Monte Carlo results. Figures 11 and 12 also show that the relative increase in the absorption coefficient estimated with the semi-infinite model is much smaller than the true increase in μ_{a2}.

D. Determination of the Optical Coefficients from Measurements on Phantoms

As described in Section 3, the optical properties of the two-layer phantoms were determined from measurements of the absolute spatially resolved reflectance on the side of the second layer of these phantoms far away from the first layer so that a semi-infinite medium could be assumed. For the second layer of phantom 2 (same material as the first layer of phantom 1) we obtained at $\lambda = 543$ nm ($\lambda = 612$ nm) $\mu_s' = 0.52$ mm^{-1}, $\mu_a = 0.024$ mm^{-1} ($\mu_s' = 0.50$ mm^{-1}, $\mu_a = 0.025$ mm^{-1}); and for the second layer of phantom 1 (same material as the first layer of phantom 2) $\mu_s' = 1.05$ mm^{-1} and $\mu_a = 0.009$ mm^{-1} ($\mu_s' = 1.05$ mm^{-1}, $\mu_a = 0.008$ mm^{-1}) (see Table 1). The measurement of phantom 2 at $\lambda = 543$ nm is shown in Fig. 13 (lower dashed curve) and that for phantom 1 in Fig. 14 (upper dashed curve). Also shown are the theoretical curves obtained from the nonlinear regression (corresponding solid curves). Figures 13 and 14 show also the measurements of the spatially resolved reflectance on the top surface of the two-layer medium for phantom 1 (upper dashed curve of Fig. 13) and phantom 2 (lower dashed curve of Fig. 14) and the corresponding theoretical curves (solid curves). The theoretical curves were calculated using the solutions of the two-layer diffusion equation of Section 2 and the optical coefficients derived from the semi-infinite measurements. This means no parameter has been fitted in this case. It can be seen in the figures that the measurements agree qualitatively with the theoretical predictions. However, the measured reflectance of the two-layered phantoms is in both cases lower than the theoretical prediction. Similar results have been obtained for the measurements at $\lambda = 612$ nm (data not shown). We also performed Monte Carlo simulations for the two-layered phantoms by using as input optical properties determined from the measurements in semi-infinite geometry. It was found that the results of the simulations were a bit closer to the experimental data, especially at distances of ~2 mm, but the measured reflectance was still smaller than the theoretical reflectance.

The effect of the second layer on the spatially resolved reflectance is evident in Figs. 13 and 14. In the case of phantom 1 the second layer causes an increase of the reflectance for all distances compared

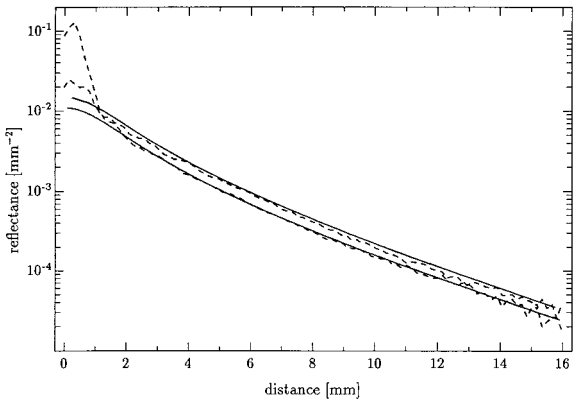

Fig. 13. Measurements of the spatially resolved absolute reflectance at the top of phantom 1 (two-layered, upper dashed curve) and at the side of phantom 2 (semi-infinite, lower dashed curve). Also shown are the nonlinear regression to the semi-infinite measurement (lower solid curve) and the theoretical curve of the two-layer measurement calculated from the known optical coefficients (upper solid curve). A He–Ne laser at $\lambda = 543$ nm was used as a light source.

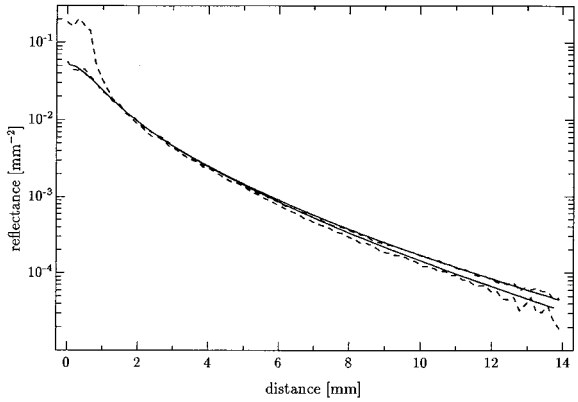

Fig. 14. Measurements of the spatially resolved absolute reflectance at the top of phantom 2 (two-layered, lower dashed curve) and at the side of phantom 1 (semi-infinite, upper dashed curve). Also shown are the nonlinear regression to the semi-infinite measurement (lower solid curve) and the theoretical curve of the two-layer measurement calculated from the known optical coefficients (upper solid curve). A He–Ne laser at $\lambda = 543$ nm was used as a light source.

with the semi-infinite case; this is because the second layer has a greater reduced scattering coefficient and a smaller absorption coefficient so that more photons are remitted back to the first layer. In contrast, the spatially resolved reflectance of the second phantom decreases compared with the semi-infinite case, because of the greater absorption of the second layer. The decrease is greater at long distances, whereas almost no difference can be seen at small distances. Because the first layer of phantom 2 is relatively thick (l = 6 mm), only a small number of the photons remitted at small distances have propagated through the second layer.

Equation 16 was used to fit the spatially resolved absolute reflectance measurements from phantom 1, and the results are summarized in Table 1. The errors in the reduced scattering coefficients range from 6% to 24% whereas those of the absorption coefficients are between 0% and 88%. Because of the experimental errors the results are worse than those obtained in Subsection 4.C. The nonlinear regression to the measurements of phantom 2 did not result in reasonable optical coefficients, because, as explained in Subsection 4.C.1, the greater thickness of the first layer results in greater errors in the derived optical coefficients. This is especially true for these experiments because the reflectance could be accurately measured only at distances to 14 mm.

Both measurements on the side (semi-infinite case) of the phantoms show values of $R(\rho)$ at small distances ($\rho \leq 1$ mm) that are much greater than the theoretical ones. This is caused by specular reflection, because the surfaces are not very flat at the sides of the phantoms. This effect is removed when measuring at the top of the phantoms (see Figs. 13 and 14), which are much smoother.

5. Conclusions

The solutions of the diffusion equation for a two-layered turbid medium presented in this article have been derived with the Fourier transform approach proposed by Dayan *et al*.[13] However, we did not introduce any approximation, and, furthermore, we solved the equations employing the extrapolated boundary condition. It has been shown for a semi-infinite medium in the steady-state, frequency, and time domains that this boundary condition results in expressions of the reflectance that are closer to Monte Carlo simulations than those based on the zero boundary condition used by Dayan *et al*.[6] The comparisons of the reflectance in the steady-state, frequency, and time domains showed that the derived solutions are close to the results obtained from two-layer Monte Carlo simulations and much better than those derived from Dayan *et al*. Thus, for many applications the reflectance (and probably the fluence rate in the tissue) calculated with these equations are exact enough to replace the time-consuming Monte Carlo simulations. Nonlinear regressions of these solutions of the diffusion equation to reflectance data obtained from the same solutions to which typical experimental noise were added showed in the steady-state and frequency domains that the absorption and the reduced scattering coefficients of the two layers and the thickness of the first layer can, in principle, be obtained. However, additional systematic errors, caused by the diffusion approximation (when compared with experiments or Monte Carlo simulations) or by the experimental apparatus, will deteriorate the results.

Although the solutions of the diffusion equation for the reflectance from a two-layered medium are quite close to the results of the transport theory, the errors in determining the optical properties caused by this approximation are greater than in the semi-infinite case. Therefore, it would be advantageous to have a solution of the transport equation for a two-layer medium fast enough to be used for determination of the optical properties. We have concentrated in this article on the determination of the absorption and reduced scattering coefficients when the thickness of the first layer is known. This information can often be obtained from general anatomy or can be determined from other methods in specific cases, e.g., from ultrasound. In the frequency domain it was found that the four optical coefficients can be determined from relative measurements of the phase and steady-state reflectance at three distances. Fantini *et al*.[30] developed an apparatus with which it is possible to perform accurate and fast measurements of the phase and steady-state reflectance at four distances. Their aim was to determine the oxygen saturation in the muscle, for example, on the forearm by use of a semi-infinite model. However, these measurements can be influenced by the overlying subcutaneous fat layer and the skin. If the thickness of the tissues above the muscle can be determined, the two-layer model presented here could be applied and should lead to improved results.

It was shown by fitting the solutions of the diffusion equation to results obtained from Monte Carlo data that the optical parameters are obtained with different accuracy. For example, for a layer thickness of l = 2 mm, μ_{s1}' could be derived within 5% from measurements in the steady-state domain, whereas μ_{s2}' could be more accurately determined in the frequency domain compared with the steady-state domain. Thus one can choose the method according to the problem that has to be investigated. For example, if the optical coefficients of the skin are required, frequency domain measurements (at least if performed at relatively small frequencies) do not seem to add useful informations. Investigations for greater thicknesses of the first layers showed that in these cases measurements in the frequency domain are superior to those performed in the steady-state domain. It was observed that the optical coefficients obtained from the two-layered model are more influenced by statistical errors than those derived with the semi-infinite model. This might be a serious disadvantage of the two-layer approach when used for monitoring physiological variables.

The results obtained in this article can *a priori* be

used only for two-layered turbid media. Biological tissue often has a multilayered structure. It must be carefully investigated to determine if it is possible to condense several tissue layers to one in order to use the two-layered model. This point is crucial for the application of the two-layered model for *in vivo* measurements. Alternatively, it is possible to extend the solution of the diffusion equation presented here to three or more layers in a straightforward manner, but the inverse problem becomes more difficult.

A major question in near-infrared spectroscopy of the adult head is whether the probing volume of the measurements is limited to the skull and skin layers or if it is possible to obtain information from the brain. Measurements on the adult head are limited by signal-to-noise to distances of approximately $\rho = 5$ cm, and the layers above the brain are ~10 mm thick.[31] Thus, this situation is comparable with those for which results are presented in Figs. 11 or 12. These figures show that the use of a semi-infinite model results in apparent changes in the absorption coefficient that are much smaller than the real changes in μ_{a2}. For the medium with $l = 10$ mm (Fig. 12), the derived absorption coefficient increases by 0.0022 mm^{-1} when μ_{a2} increases from $\mu_{a2} = 0.01$ mm^{-1} to $\mu_{a2} = 0.022$ mm^{-1}. Thus the real change in the absorption coefficient is more than five times greater than the derived change. Therefore, a multilayer model could potentially improve the measurement of hemodynamics in the adult brain.

The investigations in the time domain showed that it is possible to obtain the optical coefficients of the two layers from a measurement of the absolute reflectance at a single distance if the thickness of the first layer is known. Measurements in the time domain contain more information than those in the steady-state or frequency domains (when performed at a single frequency) and may, therefore, offer the greatest potential for the determination of the optical properties of multilayered media.

This research was supported by the National Institutes of Health grant PO1-CA43892 and the Swiss Priority Program Optics 2 (Project 423). Alwin Kienle is grateful for a postdoctoral scholarship from the German Research Society (Deutsche Forschungsgemeinschaft).

References

1. S. Homma, T. Fukunaga, and A. Kagaya, "Influence of adipose tissue thickness on near infrared spectroscopic signals in the measurement of human muscle," J. Biomed. Opt. **1,** 418–424 (1996).
2. P. J. Kirkpatrick, P. Smielewski, J. M. K. Lam, and P. Al-Rawi, "Use of near infrared spectroscopy for the clinical monitoring of adult brain," J. Biomed. Opt. **1,** 363–372 (1996).
3. A. Ishimaru, *Wave Propagation and Scattering in Random Media* (Academic, New York, 1978), Chaps. 7 and 9.
4. M. S. Patterson, B. Chance, and B. C. Wilson, "Time-resolved reflectance and transmittance for the noninvasive measurement of tissue optical properties," Appl. Opt. **28,** 2331–2336 (1989).
5. R. C. Haskell, L. O. Svaasand, T. T. Tsay, T. C. Feng, M. McAdams, and B. J. Tromberg, "Boundary conditions for the diffusion equation in radiative transfer," J. Opt. Soc. Am. A **11,** 2727–2741 (1994).
6. A. Kienle and M. S. Patterson, "Improved solutions of the steady-state and time-resolved diffusion equations for reflectance from a semi-infinite turbid medium," J. Opt. Soc. Am. A **14,** 246–254 (1997).
7. A. Kienle and M. S. Patterson, "Determination of the optical properties of turbid media from a single Monte Carlo simulation," Phys. Med. Biol. **41,** 2221–2227 (1996).
8. A. H. Hielscher, H. Liu, B. Chance, F. K. Tittel, and S. L. Jacques, "Time-resolved photon emission from layered turbid media," Appl. Opt. **35,** 719–728 (1996).
9. A. Kienle and R. Hibst, "New optimal wavelength for treatment of portwine stains?," Phys. Med. Biol. **40,** 1559–1576 (1995).
10. A. Kienle, L. Lilge, M. S. Patterson, B. C. Wilson, R. Hibst, and R. Steiner, "Investigation of multi-layered tissue with in-vivo reflectance measurements," in *Photon Transport in Highly Scattering Tissue*, S. Avrillier, B. Chance, G. J. Müller, A. V. Priezzhev, and V. V. Tuchin, eds., Proc. SPIE **2326,** 212–221 (1994).
11. S. Takatani and M. D. Graham, "Theoretical analysis of diffuse reflectance from a two-layer tissue model," IEEE Trans. Biomed. Eng. **BME-26,** 656–664 (1979).
12. J. M. Schmitt, G. X. Zhou, E. C. Walker, and R. T. Wall, "Multilayer model of photon diffusion in skin," J. Opt. Soc. Am. A **7,** 2141–2153 (1990).
13. I. Dayan, S. Havlin, and G. H. Weiss, "Photon migration in a two-layer turbid medium. A diffusion analysis," J. Mod. Opt. **39,** 1567–1582 (1992).
14. M. Keijzer, W. M. Star, and P. R. M. Storchi, "Optical diffusion in layered media," Appl. Opt. **27,** 1820–1824 (1988).
15. M. Schweiger, S. R. Arridge, M. Hiraoka, and D. T. Delpy, "The finite element model for the propagation of light in scattering media: Boundary and source conditions," Med. Phys. **22,** 1779–1792 (1995).
16. W. Cui and L. E. Ostrander, "The relationship of surface reflectance measurements to optical properties of layered biological media," IEEE Trans. Biomed. Eng. **39,** 194–201 (1992).
17. R. Nossal, J. Kiefer, G. H. Weiss, R. Bonner, H. Taitelbaum, and S. Havlin, "Photon migration in layered media," Appl. Opt. **27,** 3382–3391 (1988).
18. E. Okada, M. Firbank, and D. T. Delpy, "The effect of overlying tissue on the spatial sensitivity profile of near-infrared spectroscopy," Phys. Med. Biol. **40,** 2093–2108 (1995).
19. J. T. Bruulsema, J. E. Hayward, T. J. Farrell, M. S. Patterson, L. Heinemann, M. Berger, T. Koschinsky, J. Sandahl-Christiansen, H. Orskov, M. Essenpreis, G. Schmelzeisen-Redeker, and D. Böcker, "Correlation between blood glucose concentration in diabetics and noninvasively measured tissue optical scattering coefficient," Opt. Lett. **22,** 190–192 (1997).
20. W. H. Press, B. P. Flannery, S. A. Teukolsky, and W. T. Vetterling, *Numerical Recipes in Pascal* (Cambridge University, Cambridge, England, 1990).
21. B. W. Pogue and M. S. Patterson, "Error assessment of a wavelength tunable frequency domain system for noninvasive tissue spectroscopy," J. Biomed. Opt. **1,** 311–323 (1996).
22. A. Kienle and M. S. Patterson, "Determination of the optical properties of semi-infinite turbid media from frequency-domain reflectance close to source," Phys. Med. Biol. **42,** 1801–1819 (1997).
23. B. C. Wilson and G. Adam, "A Monte Carlo model for the absorption and flux distribution of light in tissue," Med. Phys. **10,** 824–830 (1983).
24. L. Wang, S. L. Jacques, and L. Zheng, "MCML-Monte Carlo

modeling of light transport in multi-layered tissues," Comput. Methods Programs Biomed. **47,** 131–146 (1995).
25. L. G. Henyey and J. L. Greenstein, "Diffuse radiation in galaxy," Astrophys. J. **93,** 70–83 (1941).
26. R. Graaff, M. H. Koelink, F. F. M. de Mul, W. G. Zijlstr, A. C. M. Dassel, and J. G. Aarnoudse, "Condensed Monte Carlo simulations for the description of light transport," Appl. Opt. **32,** 426–434 (1993).
27. P. R. Bevington, *Data Reduction and Error Analysis for the Physical Sciences* (McGraw-Hill, New York, 1983), Chap. 11.
28. A. Kienle, L. Lilge, M. S. Patterson, R. Hibst, R. Steiner, and B. C. Wilson, "Spatially-resolved absolute diffuse reflectance measurements for non-invasive determination of the optical scattering and absorption coefficients of biological tissue," Appl. Opt. **35,** 2304–2314 (1996).
29. R. Bays, G. Wagnières, D. Robert, J.-F. Theumann, A. Vitkin, J.-F. Savary, P. Monnier, and H. van den Bergh, "Three-dimensional optical phantom and its application in photodynamic therapy," Laser Surg. Med. **21,** 227–234 (1997).
30. S. Fantini, M. A. Franceschini-Fantini, J. S. Maier, S. A. Walker, B. Barbieri, and E. Gratton, "Frequency-domain multichannel optical detector for noninvasive tissue spectroscopy and oximetry," Opt. Eng. **34,** 32–42 (1995).
31. S. R. Arridge and M. Schweiger, "Photon-measurement density functions. Part 2: Finite-element-method calculations," Appl. Opt. **34,** 8026–8037 (1995).